Ion Partitioning at the liquid/vapor interface of a multi-component alkali halide solution: A model for aqueous sea salt aerosols

Sutapa Ghosal,[1#] Matthew A. Brown,[2] Maria J. Krisch,[2] Hendrik Bluhm,[3] Miquel Salmeron,[4] Pavel Jungwirth,[5#] John C. Hemminger*[2#]

[1]Chemistry, Materials and Life Sciences Directorate, Lawrence Livermore National Laboratory, L-231, Livermore CA 94551, USA
[2]Department of Chemistry, and AirUCI, University of California, Irvine, California 92697
[3]Chemical Sciences Division, Lawrence Berkeley National Laboratory, University of California, Berkeley, California 94551
[4]Molecular Foundry, Lawrence Berkeley National Laboratory, University of California, Berkeley, California 94720
[5]Institute of Organic Chemistry and Biochemistry, Academy of Sciences of the Czech Republic, and Center for Complex Molecular Systems and Biomolecules, Flemingovo nám. 2, 16610 Prague 6, Czech Republic

#e-mails: ghosal2@llnl.gov, pavel.jungwirth@uochb.cas.cz, jchemmin@uci.edu

Abstract

The chemistry of Br species associated with sea salt ice and aerosols has been implicated in the episodes of ozone depletion reported at Arctic sunrise. However, Br^- is only a minor component in sea salt, which has a Br^-/Cl^- molar ratio of ~0.0015. Sea salt is a complex mixture of many different species, with NaCl as the primary component. In recent years experimental and theoretical studies have reported enhancement of the large, more polarizable halide ion at the liquid/vapor interface of corresponding aqueous alkali halide solutions. The proposed enhancement is likely to influence the availability of sea salt Br^- for heterogeneous reactions such as those involved in the ozone depletion episodes. We report here ambient pressure x-ray photoelectron spectroscopy studies as well as molecular dynamics simulations showing direct evidence of Br^- enhancement at the interface of an aqueous NaCl solution doped with bromide. The experiments were carried out on samples with Br^-/Cl^- ratios in the range 0.1% to 10%. This is the first direct measurement of interfacial enhancement of Br^- in a multi-component solution with particular relevance to sea salt chemistry.

Introduction

Detailed knowledge of the surface composition of mixed salt solutions is fundamental to the understanding of chemical reactions occurring at the liquid/vapor interface of such systems. For instance, reactions of atmospheric oxidants (e.g. ozone or OH radical) at the surfaces of aqueous sea salt aerosols and particles have been implicated as a source of gas phase halogen compounds in the marine region of the troposphere.[1, 2] Correlated measurements of ground level ozone and halogen compounds in the Arctic during the spring indicate that observed episodes of significant depletion of ground level ozone concentrations are associated with gas phase chemistry of bromine compounds.[3-9] Since bromide is a minor component of sea salt (Br/Cl ~ 0.0015),[10] segregation of bromide to the surface of sea salt ice and aerosols would strongly impact the efficiency of any reactions involving Br^- at the interface.[11, 12] It is noteworthy that enrichment of bromide in the surface layer of the Arctic snow pack, possibly resulting from the ice freezing process or by atmospheric deposition of aerosols enriched in bromide, has been observed.[13] Koop et al. have suggested that sea salt aerosols are likely be liquid most of the time under polar marine boundary conditions.[12]

In previous experiments, we have shown that the liquid/vapor interface of single component aqueous solutions of KBr and KI are enriched in those halide ions (bromide and iodide respectively), whereas aqueous solutions of KF behave in agreement with classical thermodynamics in which the surface is depleted in ions.[14-16] In addition, those experiments have shown that the concentration of halide ions at the liquid/vapor interface become more significant as the anion size and polarizability are increased in the series F^-

$< Cl^- < Br^- < I^-$. Also, based on their study on a mixed solution of tetrabutylammonium iodide and tetrabutylammonium bromide Winter et al. have shown that iodide is more enhanced in the interfacial layer compared to bromide.[17] Our earlier results and the experiments of Winter et al. are also consistent with predictions from molecular dynamics (MD) simulations that take into account the polarizability of the halide ions.[18-24] With respect to atmospheric chemistry, understanding the behavior in multi-component aqueous alkali halide solutions is critical in terms of making accurate predictions concerning reactivity. For instance, in the case of aqueous sea salt aerosols, knowing the relative concentrations of Br^- versus Cl^- ions at the interface may help explain the predominance of Br^- chemistry during the Arctic spring. Previous MD simulations have predicted that in a mixed solution having equal amounts of NaBr and NaCl, Br^- exhibits preferential enhancement at the interface relative to both Cl^- and Na^+ ions as well as in comparison to the bulk Br^- concentration.[24] The results presented here provide the first experimental observation of the predicted Br^- enhancement at the solution/vapor interface of a mixed NaBr and NaCl aqueous solution. The experimental observations are directly compared with an MD simulation study of a mixed NaBr/NaCl aqueous slab with an order of magnitude more Cl^- than Br^- ions. This Br^-/Cl^- ratio of 10% is approximately equal to the anionic ratio employed in the experiment, and is also closer to the actual situation in aqueous sea salt aerosols than in the previous simulations. In one of the of experiments described here an anionic ratio of 0.1% was used which is close to the Br^-/Cl^- ratio found in natural sea water.[10]

Experimental and Computational Details

Ambient Pressure XPS

The experiments presented here used ambient pressure XPS (APPES) with synchrotron light as a source of X-rays to measure the surface composition of salt solution as a function of depth into the solution. Measurements were made at the Molecular Environmental Sciences beamline (11.0.2) of the Advanced Light Source (ALS) at Lawrence Berkeley National Laboratory.[25] The experimental apparatus utilizes a detection system similar to a prototype that is described in the literature.[26] Details of the experimental setup have been presented previously and therefore only a brief description of the sample presentation is given here. [14, 15]

Large NaCl single crystals that are uniformly doped with Br were obtained from the Crystal Growth Laboratory at University of Utah, Salt Lake City, Utah. The crystals were grown from a melt of NaCl and NaBr. This method produces high quality, uniformly doped crystals that are free of water impurities, in contrast to crystals grown from aqueous solution. The bulk compositions of two of the Br doped crystals were determined to have Br:Cl ratios of 0.07 and 0.001 by bulk elemental analysis (Desert Analytics, Arizona).[27] All salt samples were prepared by cleavage either in vacuum or air and were mechanically attached on the sample holder with TorrSeal. For measurements the spectroscopy chamber was backfilled with ~1.6 Torr water vapor. To generate a salt solution the crystal was brought to deliquescence by cooling it until the sample temperature and water vapor pressure in the chamber reached the deliquescence point of the salt and the presence of solution was observed visually. A circulating chiller and a

Peltier block were used in combination to achieve sample temperatures between -9 and -12 °C, as read by a thermocouple attached to the bottom of the salt crystal. The crystal was kept as the coldest point in the chamber, and thus was the first location to condense water. Pressure and temperature were continuously monitored to ensure that the system remained at deliquescence (pressure was read by a baratron pressure gauge). Relative humidity within the chamber was determined based on measured water vapor pressure in the chamber and sample temperature.

We measured Na(2s), Br(3d), Cl(2p), and O(1s) XP spectra at different photon energies to obtain depth profiles of Na^+, Br^-, Cl^-, and $O(H_2O_{(l)})$, relying on the fact that the surface sensitivity in XPS arises from the inelastic mean free path (which is kinetic energy dependent) of the ejected photoelectrons. By tuning the incoming X-ray energy, we can vary the photoelectron kinetic energy (PKE). The resulting signal is integrated; we collect photoelectrons from a range of sample depths varying up to the maximum accessible escape depth at any given energy. To directly compare elemental ratios, we took sets of spectra corresponding to a single probing depth (same photoelectron kinetic energy) for all elements in rapid succession on one spot on the sample.

Beam damage from the incident X-rays is a concern in the halide spectra, although the increased ionic mobility in liquids makes this less problematic in liquids than in solids. Halide spectra were always taken first in any series of data. We moved analysis spots on the sample frequently, not collecting more than one series in the same spot for the data presented here. We did not observe beam damage effects for Na(2s), and O(1s).

MD Simulations

The solution/vapor interface was modelled computationally using 1.5 ns molecular dynamics simulations (after 0.5 ns of equilibration) at 300 K of an aqueous slab containing approximately 5 M of NaCl and 0.5 M of NaBr. Simulations were performed using the AMBER 7 program package with polarizable force field for water (POL3) and ions.[18, 19, 28, 29] The induced dipoles were converged in each step using a self-consistent procedure. A slab containing 864 water molecules was enriched by 96 sodium cations, 87 chloride anions and 9 bromides and placed in a 30 x 30 x 100 $Å^3$ rectangular 3D periodic box. The smooth particle mesh Ewald method was used to account for the long range electrostatic energies and forces, with the van der Waals interactions and the real space part of the Ewald sum being truncated at 12 Å.[30].A time step of 1 fs was employed for the integration of the equations of motion. The OH bond vibrations in water were frozen using the SHAKE algorithm. [31]

Results & Discussion

Surface composition of Br^- doped NaCl single crystal vs. relative humidity. We used APPES to measure the relative ion concentrations at the free surface of Br^- doped NaCl single crystals, under different relative humidity (RH) conditions up to the sample deliquescence point. The goal was to monitor changes in the salt surface composition during the dissolution process. XP spectra of the cleaved single crystal surface were collected in the presence of water vapor. Spectra corresponding to the Br(3d), Na(2s), Cl(2p), O(1s), and C(1s) regions were acquired with a photoelectron kinetic energy of 200 eV, which corresponds to an inelastic mean free path (IMFP) probe

depth of 5-11 Å.[32] Figure 1C shows the changes in the surface Br^-/Na^+ and Br^-/Cl^- ion ratios as a function of relative humidity, for a 7% Br^- doped NaCl single crystal sample. The Br^-/Na^+ and Br^-/Cl^- ratios remained constant around average values of 0.037 (±0.003) and 0.050 (±0.006), respectively, while the relative humidity was increased in a step-wise fashion below the sample deliquescence point. At deliquescence (75% relative humidity), with the formation of a saturated solution in equilibrium with the underlying solid salt, both Br^-/Na^+ and Br^-/Cl^- ratios underwent significant increase to 0.42 and 0.65, respectively. The spectra shown in Figures 1A and 1B correspond to the dry and the deliquesced salt surface, respectively and have been charge referenced to the Na(2s) orbital set at 63.50 eV, characteristic of solid NaCl.[33] The increase in the Br^- peak area relative to Na^+ at deliquescence reflects the relative enhancement of Br^- in the saturated salt solution. The onset of Br^- enhancement begins above 50% RH, in agreement with previous laboratory based XPS measurements.[34]

Similar experiments were also carried out for the case of a 0.1% Br doped NaCl single crystal sample (Figure 2). Given the significantly lower Br^- dopant level in the 0.1% Br^- doped salt, the Br^- concentration at the dry salt surface was below the experimental detection limit. This is evident in the absence of the Br^- peak in the XP spectrum corresponding to dry salt (Figure 2A). However, at deliquescence there was an abrupt increase in the relative Br^- concentration in the resultant saturated solution which was in equilibrium with the underlying solid salt. Furthermore, the relative concentration of Br^- in the solution increased in magnitude over time. This is evidenced by the appearance of the Br^- peak in the spectrum corresponding to the deliquesced salt solution, as well as the increase in the Br^-/Na^+ and Br^-/Cl^- ratios (Figures 2B and 2C).

There are a number of studies probing the partitioning of Br^- vs. Cl^- between liquid and solid phases, in a multiphase mixed NaBr/NaCl system where both solid and solution are present.[12, 34-37] Using scanning polarization force microscopy (SPFM), we have previously shown that above 40% RH preferential solvation and segregation of Br^- ions results in the formation of bromide-rich islands and crystallites at the surface of 7% Br^- doped NaCl single crystals.[35] This phase separation can be explained in terms of the larger size of Br^- ion relative to Cl^- which leads to a lattice mismatch within the doped crystal and therefore drives the segregation of bromide. Furthermore, the solubility of NaBr in water is greater than that of NaCl.[38] All these effects can help explain the observed relative enhancement of Br^- in the saturated solution versus the solid salt in the above experiments.

Depth resolved distribution of Br^- in an aqueous NaBr/NaCl solution. Based on previous experimental work it is expected that the distribution of Br^- in mixed NaBr/NaCl solutions is inhomogeneous with Br^- concentration at the liquid/vapor interface being enhanced relative to the bulk as well as relative to Cl^- and Na^+ concentrations at the interface.[14-16] The interfacial enhancement effect has been predicted by MD simulations (see below) based on the larger polarizability of the Br^- ion with respect to Cl^- and Na^+.[24] The goal of our study has been to directly measure the relative distribution of ions as a function of depth into a mixed NaBr/NaCl solution and thereby experimentally verify the proposed enhancement. To achieve this we have made depth resolved ion distribution measurements in both a) a fully dissolved mixed NaBr/NaCl salt solution, and b) a saturated mixed NaBr/NaCl solution in equilibrium with the solid salt. In a fully dissolved NaBr/NaCl salt solution difference in solubility between NaBr and

NaCl do not contribute to the results. Therefore, in such a solution one would expect to recover the original ion concentrations in the bulk of the solution.

In the first set of experiments, the 7% Br^- doped NaCl single crystal was completely dissolved to form an unsaturated solution, by exposure to relative humidity conditions above the deliquescence point. XP spectra corresponding to Br(3d), Na(2s), Cl(2p), O(1s) and C(1s) regions, of the resulting solution, were collected at several different photoelectron kinetic energies (PKE): 200, 400, 600 eV. The use of different PKE enabled us to probe different depths into the solution, the lowest energy being the most surface sensitive (5-11 Å) and the highest being most representative of the bulk (2-3 nm). To obtain quantitative comparison between the different elements, the integrated areas of the photoelectron signal were normalized by the X-ray flux (calibrated at the ALS beamline using a photodiode of known quantum efficiency) and the theoretical subshell photoionization cross-sections.[39] The results are shown in Fig. 3 where we have plotted the Br^-/X ($X = Cl^-$ or Na^+) ratios as well as the absolute Br^- concentration (obtained using the O(1s) peak area of condensed phase liquid water) as a function of the PKE. The Br^-/X ratio and the absolute Br^- concentration decrease with increasing PKE, as would be expected for the surface enhancement of the larger, more polarizable Br^- ion. It is evident from Fig. 3 that the Br^-/Cl^- atomic ratio in the bulk (corresponding to the highest PKE) approaches the value of 0.07 in agreement with the 7% Br^- concentration of the bulk crystals used to generate the salt solution in these experiments.

In the second set of experiments we measured the depth resolved ion distributions in a saturated mixed NaBr/NaCl solution in equilibrium with the 10% Br^- doped NaCl crystal. The results are shown in Figure 4. The depth-dependent Br^-/Cl^- and Br^-/Na^+

atomic ratios were determined from the Br(3d), Cl(2p) and Na(2s) XP spectra. The Br^-/Cl^- and Br^-/Na^+ sensitivity factors were determined experimentally for each kinetic energy by measuring Br(3d), Cl(2p) and Na(2s) XP spectra on a dry (~10% relative humidity), freshly cleaved 10% Br^- doped NaCl single crystal sample with a nominal Br^-/Cl^- and Br^-/Na^+ atomic ratio of 0.11 and 0.10 respectively. The ratio of the Br(3d)/Cl(2p) and Br(3d)/Na(2s) peak areas from the deliquesced solution were then normalized by the experimentally determined sensitivity factors for each energy, yielding the Br^-/Cl^- and Br^-/Na^+ atomic concentrations as a function of depth into solution. The measured Br^-/X ($X = Cl^-$ or Na^+) ratios show the enhancement of Br^- at the solution/vapor interface relative to the bulk solution. These results are in qualitative agreement with the previous measurement as well as the predictions of MD simulation (see below).[24] A corresponding decrease in Cl^- surface concentration (shown as a plot of Cl^-/Na^+ in Figure 4C) occurs upon deliquescence, a result of the increased surface propensity of Br^- over Cl^- for mixed solutions. However, the magnitude of the Br^- enhancement relative to Cl^- or Na^+ is approximately 10 times greater in these measurements compared to the previous set of experiment involving fully dissolved salt solution. In case of the saturated solution in equilibrium with the solid salt, there are two factors that contribute to the measured ion ratios. One of the factors is the greater solubility of NaBr in water near 0 °C relative to NaCl (45 versus 26 weight %) which results in the enrichment of Br^- relative to Cl^- in the solution phase relative to the underlying solid phase.[38] The enrichment of Br^- in the solution versus the solid phase has been reported previously.[12] The second effect is the size and polarizability driven preferential enhancement of Br^- at the interface relative to the bulk of the solution. The overall greater magnitude of the measured Br^-/Cl^- ratios in

the saturated solution phase in contact with the solid salt is the result of preferential dissolution of Br^- relative to Cl^-. In summary, two separate sets of experiments with different peak area normalization protocols, both demonstrate enhancement of Br^- at the liquid/vapor interface of a mixed NaBr/NaCl solution.

Interfacial enhancement of the polarizable halogen ion has previously been demonstrated both theoretically and experimentally for single component alkali halide salts solutions.[14-24] The contribution of anion polarizability to interfacial enhancement is evident in the MD simulations where in the absence of the polarizability factor anion enhancement was not observed.[40-42] The results presented here for the multi component alkali halide salt solutions provide direct experimental evidence for relative surface enhancement of a minor component anion (Br^-) in the solution.

Comparison of experiment with simulation results.

The computed density profiles, *i.e.* the distributions of ions from the center of the slab to the water/vapor interface averaged over the MD simulation are depicted in Fig 5. We see a significant surface enhancement (and subsurface depletion) of bromide, compared to which the surface peak of chloride is strongly suppressed. Sodium cations do not penetrate all the way to the surface but, being attracted by surface-bound anions, exhibit a subsurface peak. These computational results agree qualitatively with the experiment, not only concerning the preferential enhancement of anions over cations at the interface, but also in directly confirming the greater surface effect for the larger, more polarizable anion (*i.e.*,bromide).

A more quantitative comparison between the experiments and the simulation necessitates the convolution of the molecular dynamics simulation results with an exponentially decaying experimental probe depth that would be characteristic of the APPES experiment.[32] Unfortunately, the inelastic mean free path of photoelectrons in liquids is not well understood and accurate estimates remain difficult to obtain.[43, 44] Based on the properties of neat water we estimate that at our lowest photoelectron kinetic energy (200 eV) we probe the outermost 5-11 Å, whereas at high kinetic energy (600 eV) we probe the outermost 2-3 nm of solution.[32] In addition to the density profiles from a MD simulation of a mixed solution of 5 M NaCl an 0.5 M NaBr, Figure 5 also depicts the exponentially decaying experimental probe depth function for the estimated electron inelastic mean free path (IMFP) of 11 Å for photoelectrons with 200 eV kinetic energy. Figure 6 shows a comparison of the experimentally measured Br^-/Cl^- ratio and those derived from the convolution of the simulation data with the experimental probe for photoelectron kinetic energies of 200, 400, and 600 eV. Theoretical ion densities may be converted into simulated XPS atomic ratios using the convolution integral,

$$\int e^{\left(\frac{-z}{\Gamma(PKE)}\right)}\rho(z)dz$$

for each ion, where z is the distance into the sample from the aqueous vapor interface, $\rho(z)$ is the ion density as a function of depth into solution, obtained from the results of the MD simulations, and Γ(PKE) is the IMFP of the photoelectrons which is a function of the PKE. Both experiment and simulation show a decrease of the Br^-/Cl^- ratio with electron KE with the bulk ratio (0.07 in experiment and 0.1 simulation) being virtually recovered at 600 eV. The higher Br^-/Cl^- ratio at smaller PKE clearly demonstrates preferential

surface enhancement of bromide over chloride in aqueous mixed solutions of NaBr and NaCl.

The faster decay of the Br^-/Cl^- ratio with PKE which reveals a stronger surface effect in the experiment compared to the simulation is caused by several factors. The most likely explanation for this observation is that the solution probed in the experiments is less concentrated compared to that in the simulation. The interfacial solution concentration measured in the experiment was 0.8 M compared to the 5 M solution used in the simulation (this high concentration ensured converged statistics for all ionic species). Also, the employed polarizable force field may slightly underestimate the surface enhancement of Br^- over Cl^-. Finally, the dependence of the IMFP on the PKE may be stronger than the present estimate, which would render the computational graph in Figure 6 more steep and, therefore, closer to the experiment.

Conclusions

Surface segregation is a well known phenomenon in many multi-component systems, being driven by a variety of phenomena that lead to a minimization of the surface free energy. Surface segregation of bromide in NaBr/NaCl crystals has previously been reported by our group and others.[14, 23-25] The bromide surface segregation reported in these studies can be attributed to the different solubilities of NaBr and NaCl in water, as well as heterogeneous crystal growth resulting in NaBr-rich domains. However, they do not address the specific question of Br^- enhancement at the liquid/vapor interface of a mixed NaBr/NaCl solution. We have previously demonstrated interfacial enhancement of the polarizable halide ion in a single component aqueous alkali halide solutions.[14]

Ambient aerosols are typically multi-component systems. As such, knowledge of the relative ion distribution profiles in a multi-component system is essential for understanding the reactivity at the liquid/vapor interface of such systems. The results presented here provide direct measurement of the ion distribution in a mixed NaBr/NaCl aqueous solution as a model system for sea salt aerosol. We have used ambient pressure X-ray photoelectron spectroscopy (XPS) and MD simulations to probe the ion density profiles in aqueous solutions of NaCl doped with ~10%, 7%, and 0.1% Br^-. Both experimental and simulation results show direct evidence of polarizability induced interfacial enhancement of Br^- relative to Cl^- and Na^+, and with its bulk concentration. Furthermore, our experimental results show that in the case of a saturated solution which is in equilibrium with the solid salt the measured Br^- enhancement at the liquid/vapor interface of the solution is the combined effect of – 1) solubility induced enrichment of Br^- in the solution versus the solid phase, and 2) polarizability induced interfacial enhancement of Br^- in the solution. Therefore, both effects are likely to contribute to the increased availability of sea salt bromide for heterogeneous chemistry involving sea salt ice and aerosol surfaces.

Acknowledgment

The AirUCI Environmental Molecular Sciences Institute supported this work under grant CHE 0431312 from the National Science Foundation. The ALS and the molecular environmental sciences beamline (11.0.2) are supported by the Director, Office of Science, Office of Basic Energy Sciences, Division of Chemical Sciences, Geosciences, and Biosciences and Materials Sciences Divisions of the U.S. Department

of Energy at the LBNL under contract DE-AC02-76SF00098. We gratefully acknowledge support from the Granting Agency of the Czech Republic (grant 203/07/1006) and from the Czech Ministry of Education (grant LC512). This work performed under the auspices of the U.S. Department of Energy by Lawrence Livermore National Laboratory under Contract DE-AC52-07NA27344. M.A.B. acknowledges the ALS Doctoral Fellowship program.

References

1. Knipping, E. M.; Lakin, M. J.; Foster, K. L.; Jungwirth, P.; Tobias, D. J.; Gerber, R. B.; Dabdub, D.; Finlayson-Pitts, B. J. *Science* **2000**, *288*, 301.
2. S. W. Hunt et al., J. Phys. Chem. A **2004**, 108, 11559.
3. Barrie, L. A.; Bottenheim, J. W.; Schnell, R. C.; Crutzen, P. J.; Rasmussen, R. A. Nature **1988**, 334, 138-141,.
4. Hausmann, M.; Platt, U. *J. Geophys. Res.* **1994**, 99, 25399-25413.
5. Platt, U.; Hausmann, M. *Res. Chem. Intermed*. **1994**, 20, 557-578.
6. lmpey,G . A.; Shepson, P. B.; Hastie, D. R.; Barrie, L . A.; Anlauf, K. *J. Geophys. Res.* **1997**, 102, 16005-16010.
7. Tuckermann, M.; Ackermann, R.; GOlz, C.; Lorenzen-Schmidt, H.; Senne, T.; Stutz, J.; Trost, B.; Unold, W.; Platt, U. *Tellus*, **1997,** 49B, 533-555.
8. Richter, A.; Wittrock, F. F.; Eisinger, M.; Burrows, J. P. *Geophys. Res. Lett.* **1998**, 25, 2683-2686.
9. Foster, K. L.; Plastridge, R. A.; Bottenheim, J W.; Shepson, P. B.; Finlayson-Pitts, B. J.; Spicer, C. W. *Science* **2001**, 291, 471.
10. Kester, D. R.; Ducdall, I. W.; Conners, D. N.; Pytkowicz, R. M. *Limnol. Oceanogr*. **1967**, 12, 176-179.
11. Oum, K. W.; Lakin, M. J.; Finlayson-Pitts, B. J. *Geophys. Res. Lett.* **1998**, *25*, 3923-3926.
12. Koop, T.; Kapilashrami, A.; Molina, L. T.; Molina, M. J. *J. Geophys Res*. **2000**, *105*, 26393-26402.

13. Ariya, P. A.; Hopper, J. F.; Harris, G. W. EGS XXIII General Assembly. Nice, France. April 20-24, **1998**.

14. Ghosal, S.; Hemminger, J. C.; Bluhm, H.; Mun, B. S.; Hebenstreit, E. L. D.; Ketteler, G.; Ogletree, D. F.; Requejo, F. G.; Salmeron, M. B. *Science* **2005**, *307*: 563-566.

15. Krisch, M. J.; D'Auria, R.; Brown, M. A.; Ammann, M.; Starr, D. E.; Bluhm, H.; Tobias, D. J.; Hemminger, J. C. *J. Phys. Chem. C* **2007**, *111*, 13497

16. Brown, M.A.; D'Auria, R.; Kuo, I-F W.; Krisch, M.J.; Starr, D.E.; Bluhm, H.; Tobias, D.J.; Hemminger, J.C *PCCP*, Submitted April 2008.

17. Winter, B.; Weber, R.; Hertel, I. V.; Faubel, M.; Vrbka, L.; Junwirth, P. *Chem. Phys. Lett.* **2005**, *410*, 222-227.

18. Jungwirth, P.; Tobias, D. J. *J. Phys. Chem. B* **2001**, *105*, 10468

19. Dang, L. X.; Chang, T.-M. *J. Phys. Chem. B* **2002**, *106*, 235

20. Archontis, G.; Leontidis, E.; Andreou, G. *J. Phys. Chem. B* **2005***,* 109, 17957.

21. Jungwirth, P.; Tobias, D. J. *Chem. Rev.* **2006**,106, 1259.

22. Chang, T. M.; Dang, L. X. *Chem. Rev.* **2006***,* 106, 1305.

23. Ishiyama T, Morita A. *J. Phys. Chem. C 2007,* 111, 721.

24. Jungwirth, P.; Tobias, D. J. *J. Phys. Chem. B* **2002**, *106*, 6361.

25. Bluhm, H.; Andersson, K.; Araki, T.; Benzerara, K.; Brown, G. E.; Dynes, J. J.; Ghosal, S.; Gilles, M. K.; Hansen, H.-C.; Hemminger, J. C.; Hitchcok, A. P.; Kettler, G.; Kilcoyne, A. L. D.; Kneedler, E.; Lawrence, J. R.; Leppard, G. G.; Majzlam, J.; Mun, B. S.; Myneni, S. C. B.; Nilsson, A.; Ogasawara, H.; Ogletree,

D. F.; Pecher, K.; Salmeron, M.; Shuh, D. K.; Tonner, B.; Tyliszczak, T.; Warwick, T.; Yoon, T. H. *J. Electron Spectrosc. Relat. Phenom.* **2006**, *150*, 86.

26. Ogletree, D. F.; Bluhm, H.; Lebedev, G.; Fadley, C. S.; Hussian, Z.; Salmeron, M. *Rev. Sci. Instrum.* **2002**, *73*, 3872.

27. Desert Analytics POB, Tucson, AZ 85717.

28. Case, D. A.; Pearlman, D. A.; Caldwell, J. W.; Cheatham III, T. E.; J., W.; S., R. W.; Simmerling, C. L.; Darden, T. A.; Merz, K. M.; Stanton, R. V.; Cheng, A. L.; Vincent, J. J.; Crowley, M.; Tsui, V.; Gohlke, H.; Radmer, R. J.; Duan, Y.; Pitera, J.; Massova, I.; Seibel, G. L.; Singh, U. C.; Weiner, P. K.; Kollman, P. A. *AMBER 7, University of California, San Francisco* **2002**.

29. Caldwell, J.; Kollman, P. A. *J. Phys. Chem.* **1995**, *99*, 6208.

30. Essmann, U.; Perera, L.; Berkowitz, M. L.; Darden, T. A.; Pedersen, L. G. *J. Chem. Phys.* **1995**, *103*, 8577.

31. Ryckaert, J.-P.; Ciccotti, G.; Berendsen, H. J. C. *J. Comp. Phys.* **1977**, *23*, 327.

32. Powell, C. J.; Jablonski, A. *NIST Electron Inelastic-Mean-Free-Path Database, Version 1.1* (National Institute of Standards and Technology, Gaithersburg, MD, 2000).

33. Siegbahn, K., Gelius, U., Siegbahn, H., Olson, E.; *Phys. Scripta* **1970**, 1, 272 ()

34. Ghosal, S.; Shbeeb, A.; Hemminger, J. C. *Geophys. Res. Lett.* **2000**, 27, 1879.

35. Ghosal, S.; Verdaguer, A.; Hemminger, J. C.; Salmeron, M. *J. Phys. Chem. A* **2005**, *109*, 6361.

36. Hess, M.; Krieger, U. K.; Marcolli, C.; Hithwelker, T.; Ammann, M.; Lanford, W. A.; Peter, T. *J. Phys. Chem. C* **2007**, *111*, 13497.

37. Zangmeister, C. D.; Turner, J. A.; Pemberton, J. E. *Geophys. Res. Lett.* **2001**, 28, 995.

38. Stephen, H.; Stephen, T. (Eds.) *Solubilities of lnorganic and Organic Compounds*, Pergamon Press, Oxford, 1963.

39. Yeh, J. J.; Lindau, I. *At. Data Nuc. Data Tables* **1985**, 32, 1.

40. Perera, L; Berkowitz, M. L. *J. Chem. Phys*. **1991**. 95, 1954.

41. Dang, L. X.; Smith, D. E. *J. Chem. Phys*. **1993**. 110, 1526.

42. Dang, L. X. *J. Chem. Phys*. **1999**. 99, 6950.

43. Ottosson, N.; Faubel, M.; Hertel, I. V.; Jungwirth, P.; Winter, B. *Manuscript in preparation* **2007**.

44. Winter, B.; Faubel, M. *Chemical Reviews* **2006**, *106*, 1176.

Figure captions:

Fig. 1. Ambient pressure XP spectra of a 7% bromide doped NaCl single crystal surface under dry (~5% relative humidity) conditions (A), and (B) with the formation of a solution. The Br(3d) and Na(2s) regions are shown. The spectra have been charge referenced to the Na(2s) orbital set at 63.50 eV, characteristic of solid NaCl. (C) Plot showing the ratios of Br^-/Na^+ (blue squares) and Br^-/Cl^- (open red circles) as a function of surface relative humidity. Each data point was collected on a fresh sample spot as a means to minimize the loss of halogen signal due to X-ray beam damage.

Fig. 2. Fig 2: Ambient pressure XP spectra of a 0.1% bromide doped NaCl single crystal surface under dry (~5% relative humidity) conditions (A), and (B) with the formation of a solution. The Br(3d) and Na(2s) regions are shown. The bromide dopant level in the solid single crystal is below our XPS detection level. The spectra have been charge referenced to the Na(2s) orbital set at 63.50 eV, characteristic of solid NaCl. (C) Plot showing the ratios of Br^-/Na^+ (blue squares) and Br^-/Cl^- (open red circles) as a function of relative humidity (RH). The two sets of data points at the highest RH correspond to two consecutive measurements and represent the preferential dissolution of Br^- relative to Cl^-. Each data point was collected on a fresh sample spot as a means to minimize the loss of halogen signal due to X-ray beam damage.

Fig. 3. Plots showing the measured (A) Br^-/Cl^- and (B) Br^-/Na^+ atomic ratios and the $Br^-/O(1s)$ ($H_2O_{(l)}$) ratio as a function of photoelectron kinetic energy for a completely

dissolved 7% bromide doped NaCl single crystal. The average value of multiple measurements is shown, with the error bar representative of the standard error between sample spots. Each data point was collected on a fresh sample spot as a means to minimize the loss of halogen signal due to X-ray beam damage.

Fig. 4. Plots showing the measured (A) Br^-/Cl^-, (B) Br^-/Na^+ and (C) Cl^-/Na^+ atomic ratios as a function of PKE for a saturated 7% bromide doped NaCl aqueous solution in equilibrium with the underlying solid salt. The average value of multiple measurements is shown, with the error bar representative of the standard deviation between sample spots. Each data point was collected on a fresh sample spot as a means to minimize the loss of halogen signal due to X-ray beam damage.

Fig. 5. Computed density profiles of ionic species and water from the center of the slab to the water/vapor interface together with a curve denoting the estimated experimental probe depth. The density profiles are normalized such that the integral of each of them is the same.

Fig 6. The measured and predicted Br^-/Cl^- atomic ratio as a function of photoelectron kinetic energy. The open blue circles are the experimental results while the red squares are the atomic ratio calculated from the MD simulation. The predicted atomic ratio is calculated by integration of a convolution integral for each ion.

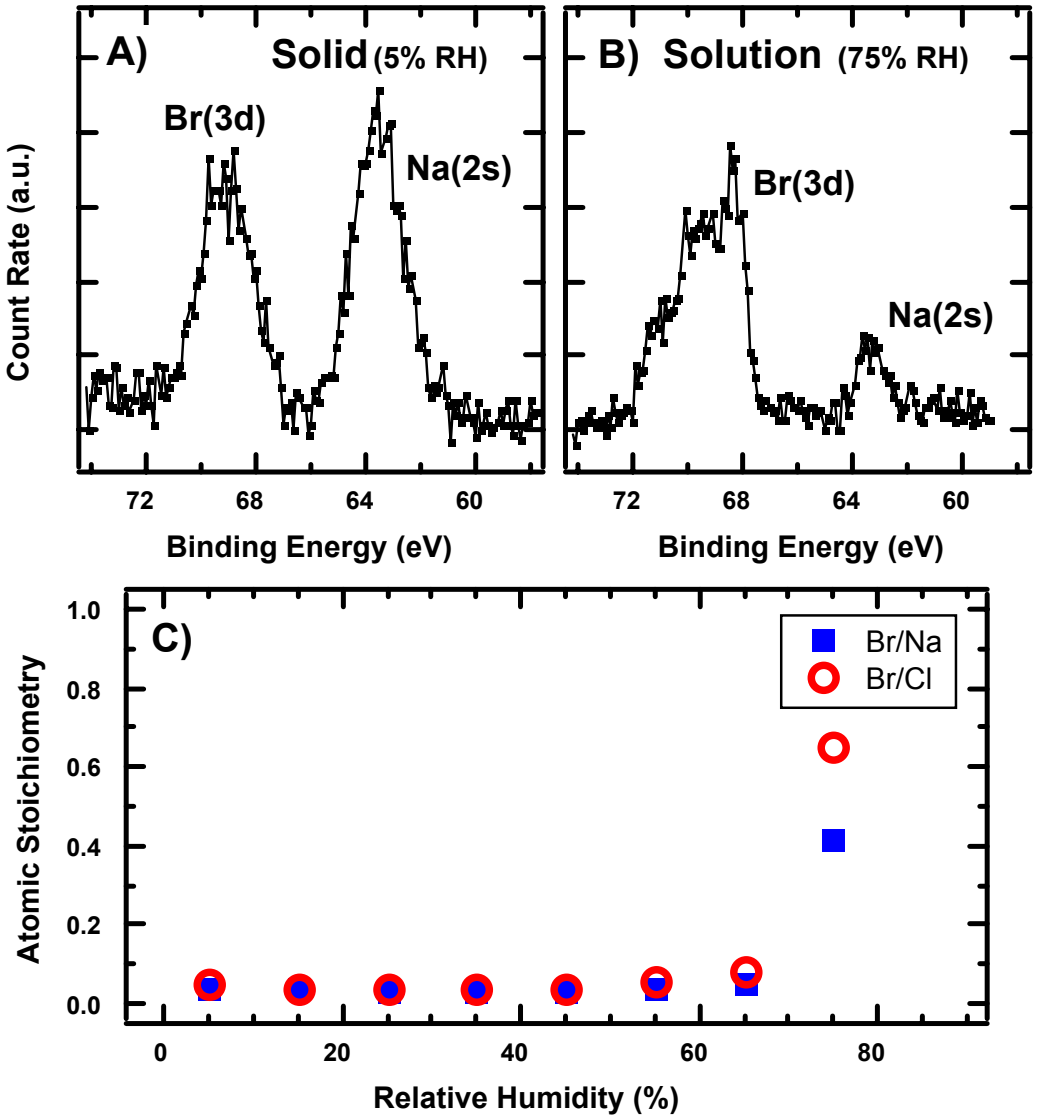

Fig 1: Ambient pressure XP spectra of a 7% bromide doped NaCl single crystal surface under dry (~5% relative humidity) conditions (A), and (B) with the formation of a solution. The Br(3d) and Na(2s) regions are shown. The spectra have been charge referenced to the Na(2s) orbital set at 63.50 eV, characteristic of solid NaCl. (C) Plot showing the ratios of Br^-/Na^+ (blue squares) and Br^-/Cl^- (open red circles) as a function of

surface relative humidity. Each data point was collected on a fresh sample spot as a means to minimize the loss of halogen signal due to X-ray beam damage.

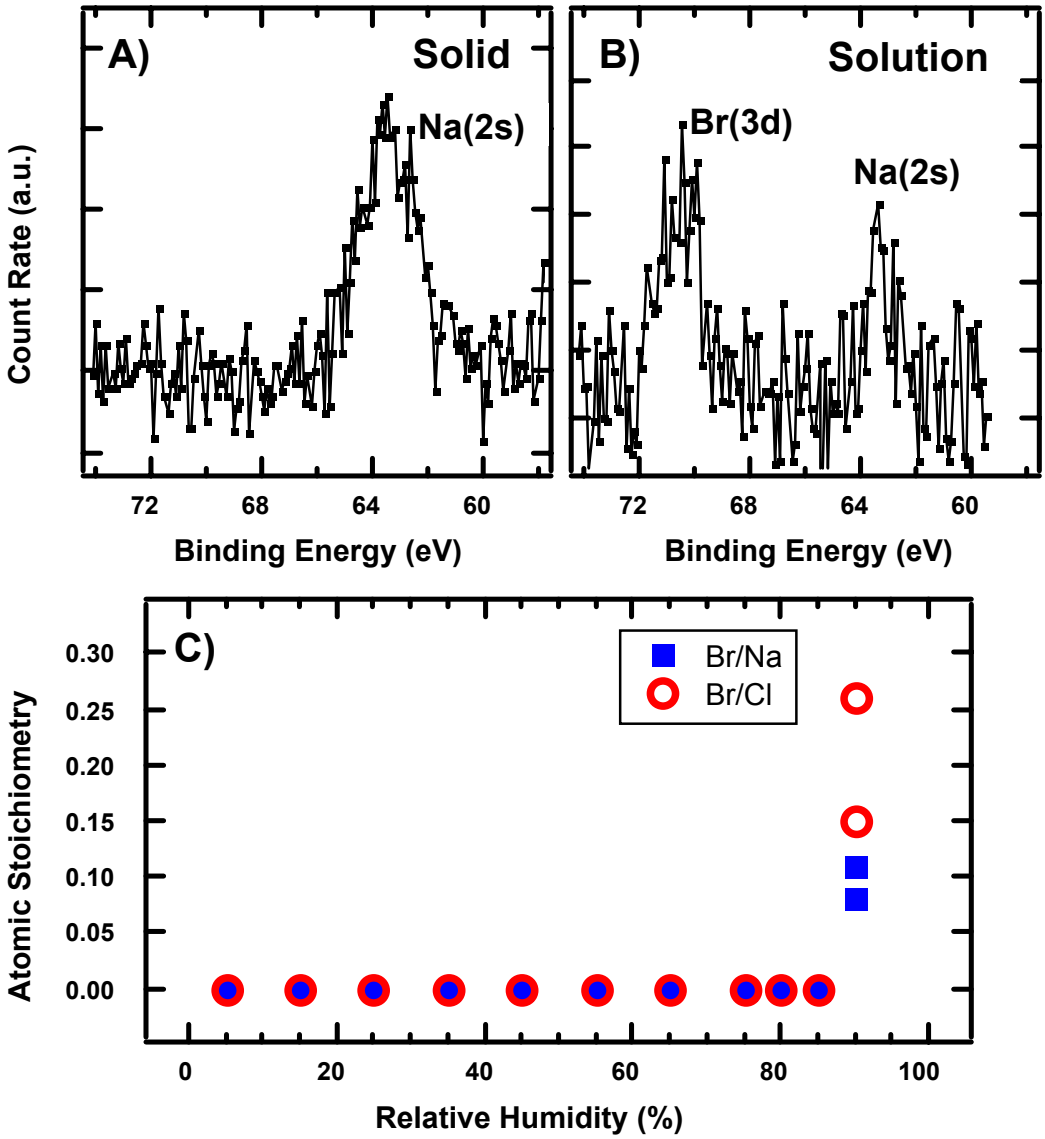

Fig 2: Ambient pressure XP spectra of a 0.1% bromide doped NaCl single crystal surface under dry (~5% relative humidity) conditions (A), and (B) with the formation of a solution. The Br(3d) and Na(2s) regions are shown. The bromide dopant level in the solid single crystal is below our XPS detection level. The spectra have been charge referenced

to the Na(2s) orbital set at 63.50 eV, characteristic of solid NaCl. (C) Plot showing the ratios of Br^-/Na^+ (blue squares) and Br^-/Cl^- (open red circles) as a function of relative humidity (RH). The two sets of data points at the highest RH correspond to two consecutive measurements and represent the preferential dissolution of Br^- relative to Cl^-. Each data point was collected on a fresh sample spot as a means to minimize the loss of halogen signal due to X-ray beam damage.

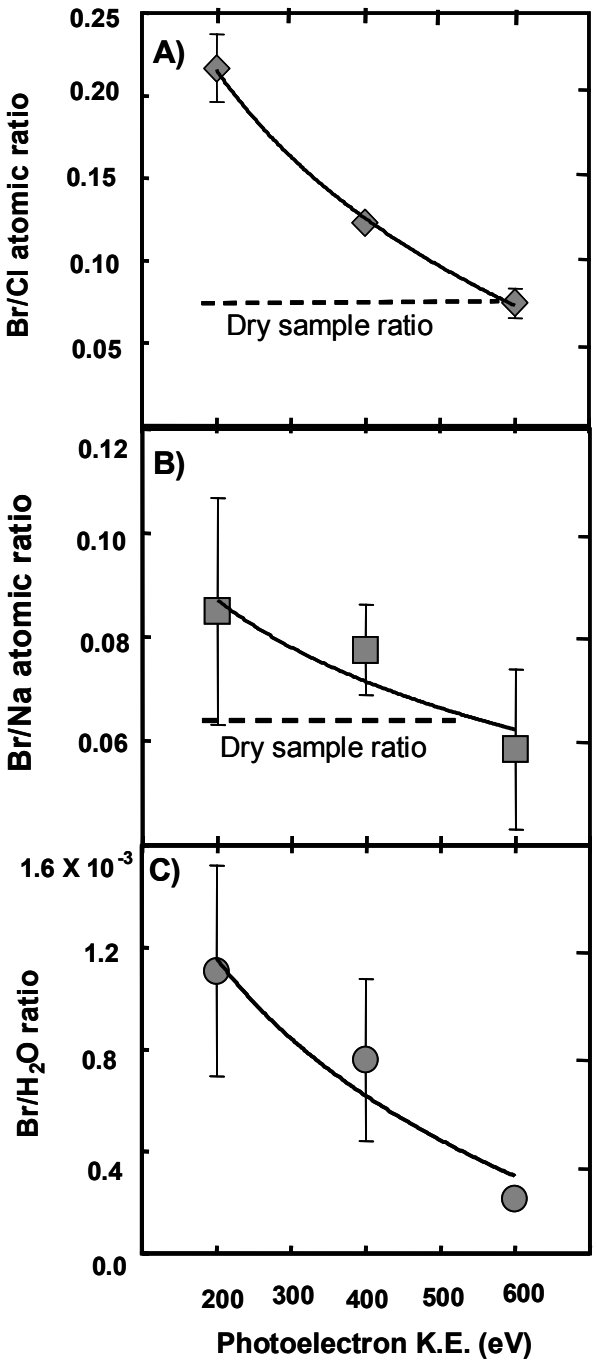
A)
Br/Cl atomic ratio
0.25
0.20
0.15
0.10
0.05
Dry sample ratio
B)
Br/Na atomic ratio
0.12
0.10
0.08
0.06
Dry sample ratio
C)
Br/H2O ratio
1.6 X 10-3
1.2
0.8
0.4
0.0
200
300
400
500
600
Photoelectron K.E. (eV)

Fig 3: Plots showing the measured (A) Br^-/Cl^- and (B) Br^-/Na^+ atomic ratios and the $Br^-/O(1s)$ ($H_2O_{(l)}$) ratio as a function of photoelectron kinetic energy for a completely dissolved 7% bromide doped NaCl single crystal. The average value of multiple measurements is shown, with the error bar representative of the standard error between sample spots. Each data point was collected on a fresh sample spot as a means to minimize the loss of halogen signal due to X-ray beam damage.

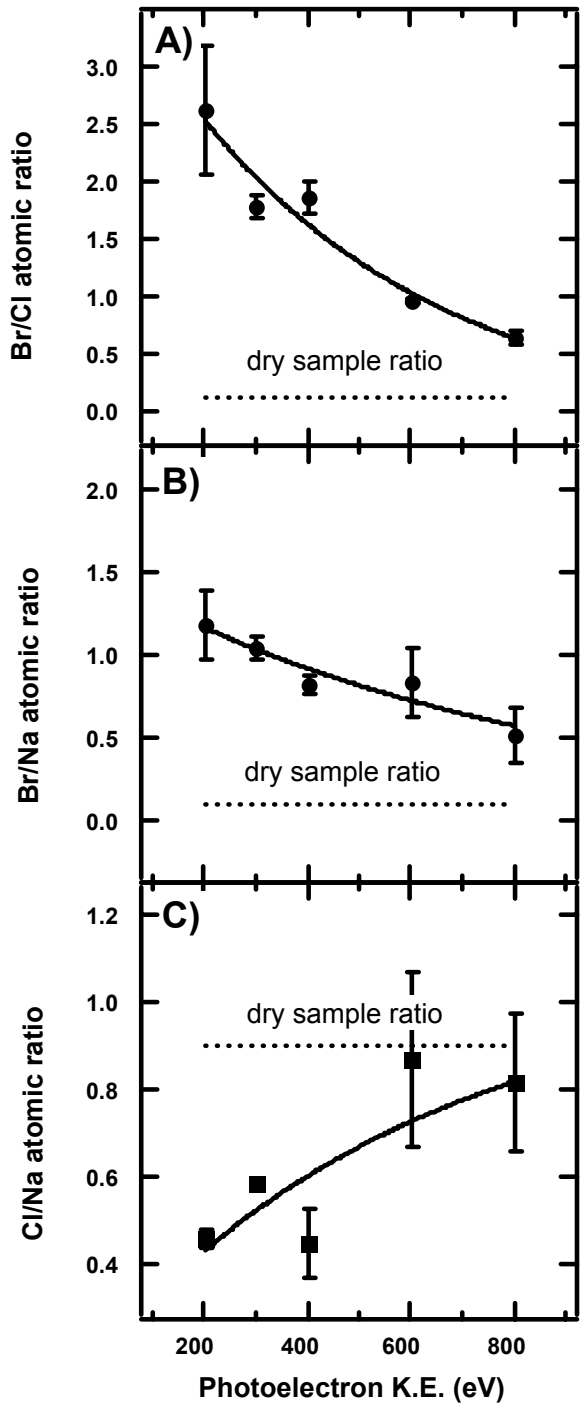

Fig 4: Plots showing the measured (A) Br^-/Cl^-, (B) Br^-/Na^+ and (C) Cl^-/Na^+ atomic ratios as a function of PKE for a saturated 7% bromide doped NaCl aqueous solution in equilibrium with the underlying solid salt. The average value of multiple measurements is

shown, with the error bar representative of the standard deviation between sample spots. Each data point was collected on a fresh sample spot as a means to minimize the loss of halogen signal due to X-ray beam damage.

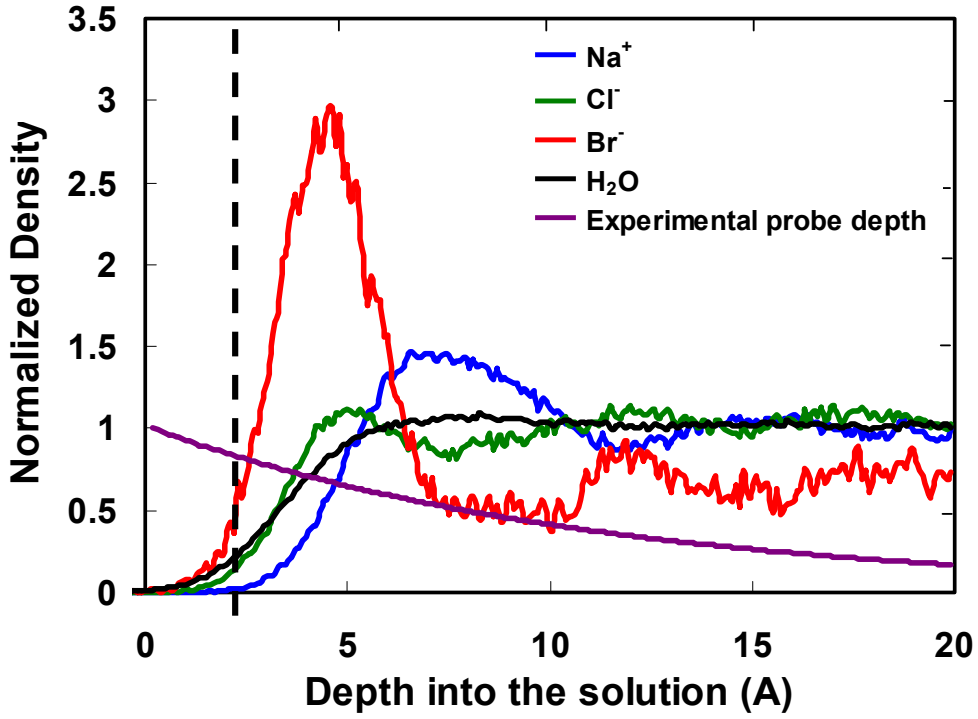

Fig. 5. Computed density profiles of ionic species and water from the center of the slab to the water/vapor interface together with a curve denoting the estimated experimental probe depth. The density profiles are normalized such that the integral of each of them is the same.

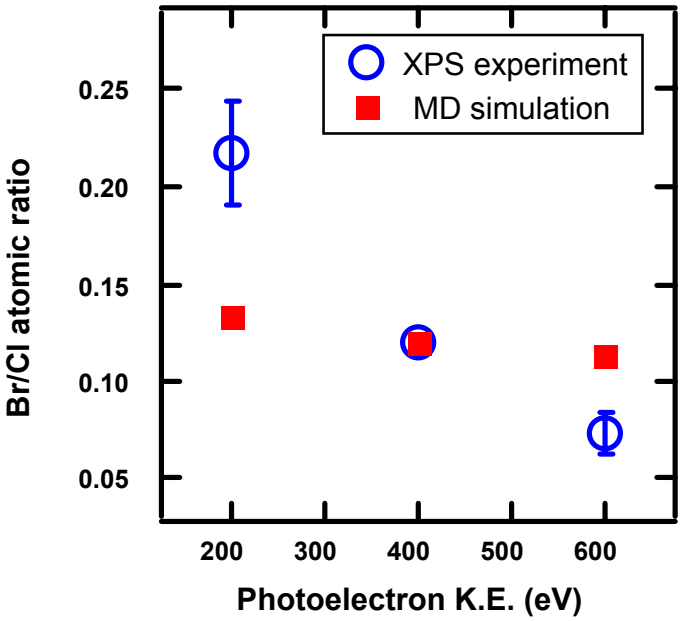

Fig 6: The measured and predicted Br^-/Cl^- atomic ratio as a function of photoelectron kinetic energy. The open blue circles are the experimental results while the red squares are the atomic ratio calculated from the MD simulation. The predicted atomic ratio is calculated by integration of a convolution integral for each ion.